

# What parameters could be extracted from Raman spectra of nanopowders?

Andrey G. Yashenkin,<sup>1,2</sup> Oleg I. Utesov,<sup>1,2,\*</sup> and Sergei V. Koniakhin<sup>3,4,†</sup>

<sup>1</sup>*Petersburg Nuclear Physics Institute NRC “Kurchatov Institute”, Gatchina 188300, Russia*

<sup>2</sup>*Department of Physics, St. Petersburg State University, St.Petersburg 199034, Russia*

<sup>3</sup>*Institute Pascal, PHOTON-N2, University Clermont Auvergne,  
CNRS, 4 Avenue Blaise Pascal, Aubière Cedex 63178, France*

<sup>4</sup>*St. Petersburg Academic University - Nanotechnology Research and Education  
Centre of the Russian Academy of Sciences, St.Petersburg 194021, Russia*

(Dated: January 27, 2023)

Analytical theory of the optical phonon line broadening in disordered nanoparticles is developed, the disorder is modelled as weak delta-correlated spatially randomized variations of atomic masses. The linewidth dependence on the mean particle size, its shape, the variance of size distribution function, the strength of disorder, as well as on the phonon quantum number is determined for both investigated regimes of separated and overlapped phonon levels, and crossover scales are determined. Analytical results are strongly supported by numerical calculations. The possibility to extract these parameters of a nanopowder of nonpolar crystal from the Raman experimental data is demonstrated and illustrated with the use of the diamond nanocrystallites serving as an example.

PACS numbers:

## INTRODUCTION

Multifarious nanoparticles, assembled in ordered arrays of quantum dots, photonic crystals, etc., [1] or existing in random formations of powders or liquid suspensions [2] are apparently the most intensively studied objects in modern physics and chemistry. Close attention to these entities is fuelled by their possible scientific and industrial applications [3–5]. Nonpolar nanocrystals, including diamond-like and semiconducting ones are very promising candidates for technological utilizations [6, 7]. Among them the special role is played by carbon nanostructures due to their good bio-compatibility, optical, electronic, and mechanical properties. Various families of nanodiamonds (detonation, laser, HPHT synthesis) inherit the outstanding properties of bulk diamond and thus are of special interest. A great amount of experimental methods, namely X-ray diffraction, dynamical light scattering, atomic force microscopy, Raman scattering, etc., are used in order to investigate these materials [8–14].

The Raman spectroscopy plays an essential role in the characterization of carbon nanomaterials. It is a precise nondestructive instrument to observe the peculiarities of collective excitations (usually optical phonons) in various materials [15, 16]. For the carbon nanostructures this method gives even more information than for other materials: distinction of  $sp^2/sp^3$ /amorphous phases [17], defectness and the number of layers in graphene, graphitization degree, and the size of nanodiamonds. And *vice versa*, among the materials studied by means of the Raman spectroscopy, the significant fraction belongs to the carbon nanostructured materials including various types of diamond nanoparticles.

Reliable analysis of the shape and the position of the

diamond crystalline Raman peak will equip us with detailed information about the nanoparticle ensemble. A simple and natural phenomenon of the finite-size quantization of the momentum in particles results in the size-dependent shift of a peak as compared to the bulk materials [18]. The full spectrum of vibrational modes which form this peak depends on the particle shape. Recently, we have developed two theories [19, 20] capable to evaluate the Raman data more precisely than the previously used phonon confinement model (PCM) [21–24]. While the current efforts of the community aim mainly to incorporate the unrealistically fine effects into the PCM [24–26, 26–29], alternative models (e.g., the local-mode model [30]) are also proposed.

The first theory (DMM-BPM) [19] is built upon the dynamical matrix method (DMM) of evaluation of vibrational modes in particles [31], with further treatment of the photon-phonon interaction induced polarization within the framework of the bond polarization model (BPM) [32, 33]. The resulting Raman spectra empirically broadened and smeared due to the particle size variation in powders constitute the main (and subsequent) Raman peaks observed experimentally. The second theory (EKFG) treats the long wavelength optical phonons which principally contribute to the main Raman peak within the effective medium approach replacing original problem by the solution of the Euclidean Klein-Fock-Gordon equation with Dirichlet boundary conditions [20]. Being supplemented by the continuous version of the BPM, after the line broadening and peak smearing procedure this theory generates the Raman peak indistinguishable from that obtained by the atomistic DMM-BPM approach.

Both these theories capture the principal features of the optical phonon spectra in diamond-like nanoparticles, including (i) existence of “Raman active” (contributing

to Raman) and “Raman silent” (not contributing) eigenmodes and (ii) presence of the first (triple-degenerate) level which provides about 2/3 of the total spectral weight being separated from the rest of the spectrum by a huge gap. The spectrum forms (iii) several “bands”, each of them could be treated as a (quasi)continuum. (iv) The structure of these bands depends on the particle shape. The theories successfully explain recent experimental data on nanodiamonds and semiconducting nanocrystals [19, 20].

The disadvantage of all current approaches for the Raman peak calculation (DMM, EKFG, local-mode, PCM) is the lack of microscopic mechanism to provide the phonon line broadening  $\Gamma$ . No microscopic explanation of this phenomenon currently exists in literature, as well (see phenomenological analysis of experiments in Refs. [34–36]). Here, DMM-BPM and EKFG theories will be used as a ground to calculate the optical phonon lifetimes  $\Gamma$  in nanocrystallites and thus the broadening of the Raman peak. Combined with the fine vibrational spectrum structure calculated with the use of the EKFG method, the knowledge of the optical phonon broadening parameters is shown to be capable to extract from the Raman spectrum (i) the mean particle size (ii) the variance of the size distribution function, (iii) the nanoparticle shape (facet number), and (iv) the strength and the concentration of lattice impurities.

Importantly, the methods developed could be applied for various crystalline nanoparticles including diamonds, Si, Ge nanoparticles, GaAs, and other quantum dots either embedded to the matrix or not. To do this, only an optical phonon dispersion, atomic masses, and parameters of the lattice defects should be modified.

We consider analytically the weak delta-correlated randomness of atomic masses as a source of spatial disorder (another source is the random spring rigidities; we believe that it would not change our principal results). We observe that the linewidths of the optical vibrational modes behave differently for separated and overlapped levels; the levels are capable to overlap due to their finite linewidths.

In the former case we used the independent levels approximation and the self-consistent Born approximation. We obtain the dependence of the linewidth  $\Gamma$  on the particle size  $L$  and disorder strength  $S$  in the form  $\Gamma \propto \sqrt{S}/L^{3/2}$ , with a prefactor depending on the quantum number of a level  $n$  and on the shape of a particle parameterized by the faceting number  $p$  (elongated particles are not considered). The disorder strength  $S$  is a product of the dimensionless impurity concentration  $c_{imp}$  and the relative mass variation  $\delta m/M$  squared,  $S = c_{imp}(\delta m/M)^2$ . For strong disorder  $\delta m/M$  should be replaced by  $\delta m/(\delta m + M)$ ; for 1% of NV-centers in nanodiamonds  $S \sim 10^{-2}$ , see Ref. [37] for details.

In the case of overlapped levels we consider first the bulk problem and then replace the  $q$ -dependence of the

linewidth by the finite size quantization rule  $q \rightarrow q_n(L, p)$  appropriate for this particle shape. Justification of this approach can be found in the body of this paper (see also Refs. [37, 38]). The linewidth obtained on this way behaves as  $\Gamma \propto S/L$ , the prefactor is  $n$  and  $p$  depended, as well.

We investigate the crossover scales between these regimes for the particle size  $L$  and for the disorder strength  $S$ .

Verifying the analytical calculations by a numerical modeling we found that the numerics strongly supports our conclusions. Furthermore, we fitted the data of Ref. [39] with the use of our theory thus proving the capability of this approach to retrieve from the experiment such characteristics of a nanopowder of nonpolar crystal as the mean particle size  $L$ , the standard deviation of the size distribution function  $\delta L$ , the strength of disorder  $S$ , and to estimate the faceting number  $p$ .

Details, extensions and generalizations of this research will be published elsewhere [37, 38].

## ANALYTICAL INVESTIGATION

The Hamiltonian of elastic medium reads

$$\mathcal{H} = \sum_l \frac{p_l^2}{2M_l} + \frac{1}{2} \sum_{ll'} \mathcal{K}_{ll'} (\mathbf{r}_l - \mathbf{r}_{l'})^2, \quad (1)$$

where the first sum describes the kinetic energy of the atoms with masses  $M_l$  packed in a lattice. These atoms are connected by the springs with rigidities  $\mathcal{K}_{ll'}$ , the elastic energy being proportional to the squared difference of the atomic displacements  $\mathbf{r}_l$  from the lattice sites  $\mathbf{R}_l$ . We incorporate the disorder via the spatial randomness of atomic masses  $M_l$  characterized by the mean value  $M = \langle M_l \rangle$  and the variation  $\delta m_l$  with zero average  $\langle \delta m_l \rangle = 0$  and delta-functional pairwise correlator  $\langle \delta m_l \delta m_{l'} \rangle / M^2 = S \delta_{ll'}$ . Disorder enters the Hamiltonian  $\mathcal{H}$  as follows:

$$\mathcal{H}_{imp} = - \sum_l \delta m_l \frac{p_l^2}{2M^2}. \quad (2)$$

Let  $\{\Psi_n(\mathbf{R}_l)\}_{n=1}^{3N}$  be a set of normalized vibrational eigenmodes for the nanoparticle of given shape and size, where  $N$  is the number of atoms in a particle,  $n$  is the generalized quantum number, and  $\omega_n$  are the corresponding eigenfrequencies. For a diamond-like crystal the atomic displacements  $\mathbf{r}_l$  and the momenta  $\mathbf{p}_l$  are given by

$$\begin{aligned} \mathbf{r}_l &= \frac{1}{\sqrt{2M}} \sum_n \frac{\Psi_n(\mathbf{R}_l)}{\sqrt{\omega_n}} (b_n + b_n^\dagger) \\ \mathbf{p}_l &= \frac{i\sqrt{M}}{\sqrt{2}} \sum_n \Psi_n(\mathbf{R}_l) \sqrt{\omega_n} (b_n^\dagger - b_n). \end{aligned} \quad (3)$$

Here  $b_n^\dagger$  ( $b_n$ ) are the bosonic creation (annihilation) operators in the basis  $\{\Psi_n(\mathbf{R}_l)\}$ ; the generalization onto more complex crystals is straightforward. Plugging Eqs. (3) into Eqs. (1) and (2) we rewrite our Hamiltonian in the form  $\mathcal{H} = \mathcal{H}_{ph} + \mathcal{H}_{imp}$ , where  $\mathcal{H}_{ph}$  represents the free phonons

$$\mathcal{H}_{ph} = \sum_n \omega_n (b_n^\dagger b_n + 1/2), \quad (4)$$

and  $\mathcal{H}_{imp}$  describes the phonon-impurity interaction

$$\mathcal{H}_{imp} = \frac{1}{4} \sum_{l,n,n'} \frac{\delta m_l}{M} \Psi_n(\mathbf{R}_l) \cdot \Psi_{n'}(\mathbf{R}_l) \sqrt{\omega_n \omega_{n'}} (b_n^\dagger - b_n)(b_{n'}^\dagger - b_{n'}). \quad (5)$$

Defining the phonon propagator  $D_n(\omega)$  as the Green's function for the operators  $\phi_n = i(b_n^\dagger - b_n)$  we get

$$D_n(\omega) = \frac{2\omega_n}{\omega^2 - \omega_n^2 - 2\omega_n \Pi_n(\omega)}, \quad (6)$$

where the self energy  $\Pi_n(\omega)$  after the impurity averaging obtains the form:

$$\Pi_n(\omega) = \frac{S\omega_n}{16} \sum_{l,n'} [\Psi_n(\mathbf{R}_l) \cdot \Psi_{n'}(\mathbf{R}_l)]^2 \omega_{n'} D_{n'}(\omega). \quad (7)$$

We shall use the self-consistent Born approximation keeping the phonon self-energy  $\Pi_{n'}(\omega)$  on the r.h.s. of Eq. (7) nonzero (otherwise,  $\text{Im} \Pi_n(\omega) = 0$ ). When the levels are separated, the main contribution to this equation comes from the term with  $n' = n$ . It yields

$$\Pi_n(\omega) = \frac{\omega^2 - \omega_n^2 - \sqrt{(\omega^2 - \omega_n^2)^2 - \frac{16c_n^2(n,p)S\omega_n^4}{N}}}{4\omega_n}, \quad (8)$$

where  $c_n^2(p) = N \sum_l [\Psi_n(\mathbf{R}_l)]^4 / 16$ .

When the square root in Eq. (8) is imaginary it determines the semi-circle law for the density of states (cf. Ref. [40]). Using the on-shell approximation  $\omega = \omega_n$  in Eq. (8) we obtain the phonon linewidth in the form:

$$\Gamma_n(L, S, p) = \omega_n \mu_n(p) \sqrt{S} \left(\frac{a}{L}\right)^{3/2}. \quad (9)$$

Here  $a$  is the lattice parameter,  $\mu_n(p) = c_n(p) \sqrt{P^3(p)/2}$ , and  $P(p)$  converts the linear size of a particle with faceting number  $p$  (for cubic particles it is the cube edge) into the diameter of a sphere with the same amount of atoms. The factor  $\mu_n(p)$  is calculated analytically for cubic, spherical, and cylindrical particles and numerically for other particle shapes.

Eq. (9) constitute our first result. It reveals the unusual dependence of the phonon linewidth on the particle size,  $\Gamma \sim L^{-3/2}$ , and on the disorder strength,  $\Gamma \sim \sqrt{S}$ , as well as its quantum number and particle shape dependence via the parameter  $\mu_n(p)$  which this quantity demonstrates in the regime of separated levels.

The approach we utilized above is similar to the self-consistent theories of disordered electrons [40–42].

Now we investigate the case of overlapped levels arising with the growth of  $L$  and/or  $S$ . In order to proceed with this regime we shall use the following approximation. Assuming that the plane waves

$$\Psi_n(\mathbf{R}_l) = \frac{\mathbf{P}_q}{\sqrt{N}} e^{i\mathbf{q}\mathbf{R}_j} \quad (10)$$

properly capture the main features of the overlapped (and therefore extended) vibrational eigenmodes we consider the bulk problem. Then we exploit the  $q$ -dependence of the result using the quantization rule  $q \rightarrow q_n(L, p)$  peculiar for this particle shape. Here  $\mathbf{P}_q$  is the phonon polarization and  $q_n(L, p)$  is the discrete phonon momentum.

Repeating in the basis of plane waves the derivation made above one arrives to the phonon propagator

$$D(\omega, \mathbf{q}) = \frac{2\omega_q}{\omega^2 - \omega_q^2 - 2\omega_q \Pi_q(\omega)}. \quad (11)$$

with the self energy

$$\Pi_q(\omega) = \frac{S\omega_q}{16N} \sum_{\mathbf{k}} \omega_{\mathbf{k}} D(\omega, \mathbf{k}). \quad (12)$$

It is sufficient to take the Green's function on the right-hand side of Eq. (12) in its bare form,  $-2\omega_q \Pi_q(\omega) \rightarrow i\delta$ .

The dispersion of the long wavelength optical phonons contributing to the Raman peak reads:

$$\omega_q \approx \omega_0 - \alpha q^2 = \omega_0 [1 - F(qa)^2], \quad (13)$$

where  $F$  is the spectrum flatness parameter (for diamond,  $F \approx 0.008$ ). The spectrum of finite-size particles is given by  $\omega_n \approx \omega_0 - \alpha q_n^2$ .

Evaluating Eq. (12) at  $\omega \sim \omega_q$  we get

$$\Pi_q(\omega) = -\frac{Sa^3\omega_q}{64\pi\alpha^{3/2}} \omega \sqrt{\omega - \omega_0}. \quad (14)$$

We absorbed into  $\omega_0$  the constant contribution to  $\text{Re} \Pi_q(\omega)$  stemming from the upper limit of integration in Eq. (12). Sharp nonanalytic frequency dependence of this self-energy came from the van Hove singularity in the density of states of optical phonons. It leads to the strong asymmetry of the lineshape [37]. Ignoring this asymmetry within the on-shell approximation  $\omega = \omega_q$  one finds:

$$\Gamma_q = \omega_q \frac{S}{32\pi F} (qa). \quad (15)$$

Applying to Eq. (15) the quantization rule  $q \rightarrow q_n(L, p)$  one obtains (cf. Ref. [34]):

$$\Gamma_n(L, S, p) = \omega_n \nu_n(p) S \frac{a}{L}. \quad (16)$$

Here  $\nu_n(p) = c'_n(p)/32F$  is the coefficient strongly dependent on the quantum number  $n$  via the factor  $c'_n(p)$  to be determined numerically for any nontrivial particle shape. With increasing of  $n$  the linewidth increases, as well. In particular, for cubic particles we have

$$\frac{\Gamma(L, S, \mathbf{n}, 6)}{\Gamma(L, S, \mathbf{1}, 6)} = \frac{|\mathbf{n}|}{\sqrt{3}}, \quad (17)$$

where  $\mathbf{n} = (n_x, n_y, n_z)$  is the quantum number describing the size quantization in a cubic box and  $\mathbf{1} = (1, 1, 1)$ .

Eq. (16) constitute our second result. It demonstrates that the linewidths of overlapped and separated levels are qualitatively different: we observe  $\Gamma \sim 1/L$  instead of  $\Gamma \sim 1/L^{3/2}$  and  $\Gamma \sim S$  instead of  $\Gamma \sim \sqrt{S}$ .

Both evaluations have been performed for nondegenerate spectral lines. The results for degenerate levels contain additional multipliers  $g_n$  which should be calculated (either analytically or numerically) for any specific particle shape (for details, see Refs. [37, 38]).

Let us estimate the crossover particle size between separated and overlapped regimes for  $\Gamma$ . Neglecting shape and quantum number dependent coefficients we obtain

$$\mathcal{L}_c \sim \frac{a}{S}. \quad (18)$$

Notice that the linewidth reaches the interlevel distance on the same spatial scale  $\mathcal{L}_c$ . Physically, in particles with  $L \sim \mathcal{L}_c$  the phonon lifetime  $1/\Gamma$  coincides with the time for phonon to traverse this particle ballistically (cf. with the Thouless time for diffusive disordered electrons [43]).

Fixing  $L$  one can introduce the crossover disorder strength which divides separated and overlapped regimes:

$$S_c \sim \frac{a}{L}. \quad (19)$$

## NUMERICAL INVESTIGATION

We support our analytical findings by proper numerics employing the exact diagonalization of the dynamical matrix with the Gaussian disorder. The eigenmodes  $|\varepsilon\rangle$  obtained in that way are utilized when calculating the broadening for the  $n$ -th mode of a pure particle. Averaging over disorder is realized with the use of the formula:

$$\overline{\sum_{\varepsilon} \delta(\omega - \varepsilon) |\langle n | \varepsilon \rangle|^2}, \quad (20)$$

the overline stands for averaging. Then we fit the spectral lines by the Lorentzians. We averaged over several hundreds configurations for each particle size/disorder strength.

As usually in disordered systems, the solution of the eigenproblem for any particular realization of disorder yields real (albeit, disorder modified) eigenfrequencies

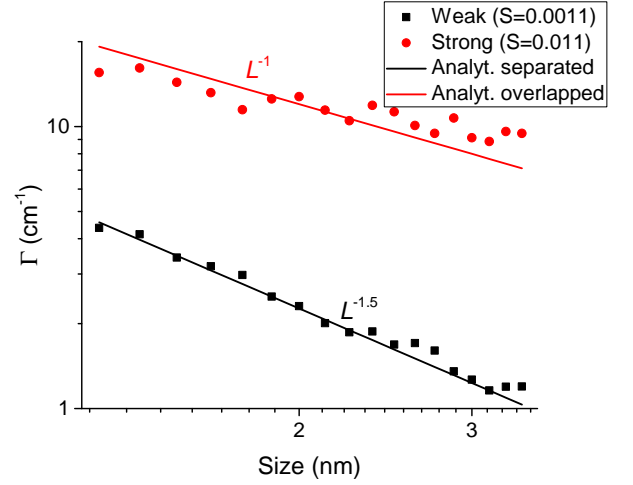


FIG. 1: The phonon linewidth  $\Gamma_1$  in a spherical nanodiamond plotted as a function of the particle size  $L$  for two disorder strengths  $S = 0.0011$  (black squares) and  $S = 0.011$  (red dots). The range of  $L$  shown in this Figure corresponds to the regime of separated levels in the former case and to the regime of overlapped levels in the latter one. The lines represent predictions of the analytical theory.

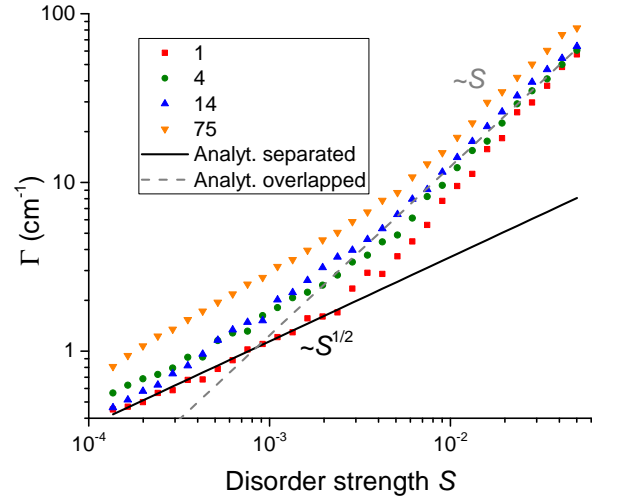


FIG. 2: The phonon linewidth  $\Gamma_n$  plotted as a function of the disorder strength  $S$  for several phonon eigenmodes ( $n = 1, 4, 14, 75$ ) of a spherical 3 nm nanodiamond. Solid and dashed lines show the analytical predictions for the first mode in separated and overlapped regimes, respectively. The highest phonon modes have broader lines. Both the functional dependencies and the crossovers are clearly seen.

and eigenfunctions. The broadening arises upon the averaging due to non-equivalence of disorder realizations; for particles, even the number of impurities in a particle fluctuates around its mean value.

In Fig. 1 we depict the comparison of our numerical and analytical results for the phonon linewidth as a func-

tion of particle size in both regimes of separated and overlapped levels whereas Fig. 2 demonstrates the linewidth dependence on the disorder strength. We emphasize a very good agreement between the analytics and the numerics including the prefactors, functional dependencies and crossovers visible in these Figures.

The theory of the phonon line broadening developed in the present paper accomplishes the more general approach of Refs. [19] and [20] providing the microscopic mechanism of the line broadening which incorporates the shape and quantum number dependence of the linewidth. It yields a possibility to build up the regular method of analyzing the Raman spectra of nanopowders of nonpolar crystals more reliably and precisely than the previously used ones. This method allows us to extract four parameters from the Raman peak shape and position, namely (i) the mean particle size in a powder  $L$ , (ii) the standard deviation of size distribution function  $\delta L$ , (iii) the disorder strength parameter  $S$ , and, hopefully, (iv) particle shape parameterized by the faceting number  $p$ . The thorough analysis of a Raman experiment should include the effects of asymmetry of phonon lines and the more detailed discussion of all possible sources of broadening. In the present paper we undertake the simplified version of such analysis re-examining the experimental data of Ref. [39] with the use of the EFKG method for overlapped levels, see Fig. 3. We observe that our microscopic theory which predicts the linewidths varying with the phonon quantum number and with the particle shape provides much better fit than the fit with empirical  $\Gamma$  equal for all phonon modes. Furthermore, we take five different particle shapes, namely the sphere, the truncated octahedron, the dodecahedron, the octahedron, and the cube. We observe that the log-normal distribution fits this experiment much better than the Gaussian. The best fit provides the following reliable values for three parameters:  $L \approx 2.6$  nm,  $\delta L \approx 1.0$  nm, and  $S \approx 0.03$ , where  $L$  and  $\delta L$  are extracted from the parameters of the log-normal distribution function. Concerning the faceting parameter  $p$  we observe that the cube ( $p = 6$ ) and the octahedron ( $p = 8$ ) yield very close values for  $\chi^2$  so we could not judge confidently about the particle shape concluding only that the number of facets  $p \simeq 6 - 8$  is not large. The possibility to perform such analysis is the third result of this paper. We believe that the more accurate Raman data and/or the more accurate microscopic DMM-BPM method will allow us to determine the particle shape more precisely.

## DISCUSSION AND CONCLUSIONS

The disorder parameter  $S = c_{imp}(\delta m/M)^2$  ( $c_{imp}U^2$  for strong impurities) extractable from our data analysis is a product of two characteristics, each of them being of the particular interest *per se*. Therefore, for the

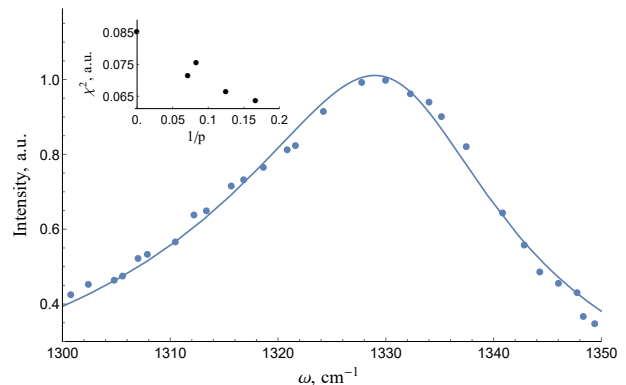


FIG. 3: The EFKG model [20] fit for the experimental Raman spectrum [39] of a nanodiamond powder, the levels supposed to be overlapped. Solid blue line corresponds to the spectrum theoretically calculated for the log-normal distribution of cubic particles with  $L \approx 2.6$  nm,  $\delta L \approx 1.0$  nm, and  $S \approx 0.03$ . The inset shows  $\chi^2$  of the best fits obtained for spheres ( $p = \infty$ ), truncated octahedra ( $p = 14$ ), dodecahedra ( $p = 12$ ), octahedra ( $p = 8$ ), and cubes ( $p = 6$ ).

comprehensive characterization of a nanopowder our theory should be supplemented by the proper analysis of its chemical composition. Some conclusions, however, could be drawn right now. First, the obtained value  $S \approx 0.03$  is too large to be explained by the isotopic disorder: for  $c_{imp} \sim 10^{-2}$  (1%) and  $\delta m/M = 1/12$  one obtains  $S \sim 10^{-4}$ . Furthermore, it is evident that for the reasonable concentration of impurities  $c_{imp} \sim 10^{-3} - 10^{-1}$  only the strong scatterers could provide the desired value of  $S$ . There are two following attractive candidates for this role in diamonds, the famous NV (nitrogen + vacancy) centers and the silicon + vacancy complexes, both of them include the vacancy which in our theory works as an infinite repulsive on-site potential. The typical concentration of the nitrogen in diamonds  $c_{imp} \sim 1 - 3\%$  and the estimated value of  $U$  for NV centers are capable to provide the value  $S \approx 0.03$ ; however, this issue deserves a more detailed treatment.

Our theory deals with the elastic processes of the phonon scattering by disorder, and, therefore, with Raman spectra at low temperatures. It is interesting to investigate this issue at higher temperatures when the inelastic processes of the phonon scattering by each other could modify the situation. Here we just mention the intriguing possibility to observe the localization-delocalization temperature crossover induced by the many-body localization effects predicted in Refs. [44, 45] for an electron counterpart (interacting electrons in a quantum dot) of present problem.

Although the presentation of this paper has been focused on the interpretation of Raman experiment, our results could be applied for the treatment of the phonon lifetime in other systems with restricted geometry such as quantum dots and short quantum wires.

To conclude, we investigated the impurity-induced broadening of levels of vibrational eigenmodes in nanopowders of nonpolar crystals and incorporated this issue into the more complex problem of the Raman peak evaluation in these materials. The disorder is chosen in the form of a weak delta-correlated spatial variation of atomic masses. Our analytical calculations demonstrate that the linewidths are essentially different for separated and overlapped phonon levels. In the latter case they reveal the linear dependence on the impurity strength  $S$ ; also, they are inversely proportional to the particle size  $L$ , providing  $\Gamma \propto S/L$ . In the former case they behave as  $\Gamma \propto \sqrt{S}/L^{3/2}$ . Both prefactors are found to be specifically shape and quantum number dependent. The crossover between these two regimes occurs when the particle size reaches the phonon inelastic mean free path. These analytical results are strongly supported by our numerics. We also demonstrated that our theory of the Raman peak shape and its position allows us to extract confidently from the Raman data three important microscopic parameters such as the mean particle size, the variance of the particle size distribution function, the strength of intrinsic disorder, and to estimate the effective faceting number parameterizing the particle shape.

### Acknowledgments

The authors are thankful to Igor Gornyi for valuable comments. This work is supported by the Russian Science Foundation (Grant No. 19-72-00031).

### Data availability

The data supporting our findings are available from the corresponding authors upon reasonable request.

---

\* Electronic address: utiosov@gmail.com

† Electronic address: kon@mail.ioffe.ru

- [1] J. Roh, Y.-S. Park, J. Lim, and V. I. Klimov, *Nature Communications* **11**, 1 (2020).
- [2] P. Geiregat, D. Van Thourhout, and Z. Hens, *NPG Asia Materials* **11**, 1 (2019).
- [3] M. Veldhorst, J. Hwang, C. Yang, A. Leenstra, B. de Ronde, J. Dehollain, J. Muhonen, F. Hudson, K. Itoh, A. Morello, et al., *Nature nanotechnology* **9**, 981 (2014).
- [4] S. V. Kidalov and F. M. Shakhov, *Materials* **2**, 2467 (2009).
- [5] Y. Xia, H. Yang, and C. T. Campbell, *Nanoparticles for catalysis* (2013).
- [6] K. D. Behler, A. Stravato, V. Mochalin, G. Korneva, G. Yushin, and Y. Gogotsi, *ACS nano* **3**, 363 (2009).
- [7] V. Pichot, M. Guerchoux, O. Muller, M. Guillevic, P. Fioux, L. Merlat, and D. Spitzer, *Diamond and Related Materials* **95**, 55 (2019).
- [8] R. Pecora, *Journal of nanoparticle research* **2**, 123 (2000).
- [9] B. Chu, *Laser light scattering: basic principles and practice* (Courier Corporation, 2007).
- [10] S. Mourdikoudis, R. M. Pallares, and N. T. Thanh, *Nanoscale* **10**, 12871 (2018).
- [11] S. Koniakhin, I. Eliseev, I. Terterov, A. Shvidchenko, E. Eidelman, and M. Dubina, *Microfluidics and Nanofluidics* **18**, 1189 (2015).
- [12] S. Koniakhin, N. Besedina, D. Kirilenko, A. Shvidchenko, and E. Eidelman, *Superlattices and Microstructures* **113**, 204 (2018).
- [13] P. A. Hassan, S. Rana, and G. Verma, *Langmuir* **31**, 3 (2015).
- [14] D. Segets, *KONA Powder and Particle Journal* p. 2016012 (2016).
- [15] M. Cardona and R. Merlin, in *Light Scattering in Solid IX* (Springer, 2006), pp. 1–14.
- [16] C. S. Kumar, *Raman spectroscopy for nanomaterials characterization* (Springer Science & Business Media, 2012).
- [17] A. C. Ferrari and J. Robertson, *Philosophical Transactions of the Royal Society of London. Series A: Mathematical, Physical and Engineering Sciences* **362**, 2477 (2004).
- [18] A. Meilakhs and S. Koniakhin, *Superlattices and Microstructures* **110**, 319 (2017).
- [19] S. V. Koniakhin, O. I. Utesov, I. N. Terterov, A. V. Siklitskaya, A. G. Yashenkin, and D. Solnyshkov, *The Journal of Physical Chemistry C* **122**, 19219 (2018), URL <https://doi.org/10.1021/acs.jpcc.8b05415>.
- [20] O. I. Utesov, A. G. Yashenkin, and S. V. Koniakhin, *The Journal of Physical Chemistry C* **122**, 22738 (2018), URL <https://doi.org/10.1021/acs.jpcc.8b07061>.
- [21] H. Richter, Z. Wang, and L. Ley, *Solid State Communications* **39**, 625 (1981).
- [22] I. Campbell and P. M. Fauchet, *Solid State Communications* **58**, 739 (1986).
- [23] K. W. Adu, H. Gutierrez, U. Kim, G. Sumanasekera, and P. Eklund, *Nano letters* **5**, 409 (2005).
- [24] G. Faraci, S. Gibilisco, P. Russo, A. R. Pennisi, and S. La Rosa, *Physical Review B* **73**, 033307 (2006).
- [25] S. Osswald, V. Mochalin, M. Havel, G. Yushin, and Y. Gogotsi, *Physical Review B* **80**, 075419 (2009).
- [26] V. I. Korepanov and H.-o. Hamaguchi, *Journal of Raman Spectroscopy* **48**, 842 (2017).
- [27] V. I. Korepanov, H. o Hamaguchi, E. Osawa, V. Ermolenkov, I. K. Lednev, B. J. Etzold, O. Levinson, B. Zousman, C. P. Epperla, and H.-C. Chang, *Carbon* **121**, 322 (2017), ISSN 0008-6223, URL <http://www.sciencedirect.com/science/article/pii/S0008622317305791>.
- [28] J. Zi, K. Zhang, and X. Xie, *Physical Review B* **55**, 9263 (1997).
- [29] W. Ke, X. Feng, and Y. Huang, *Journal of Applied Physics* **109**, 083526 (2011).
- [30] Y. Gao and P. Yin, *Diamond and Related Materials* **99**, 107524 (2019).
- [31] M. Born and K. Huang, *Dynamical theory of crystal lattices* (Clarendon press, 1954).
- [32] J. Martin and S. Montero, *The Journal of Chemical Physics* **80**, 4610 (1984),

- <http://dx.doi.org/10.1063/1.446545>, URL <http://dx.doi.org/10.1063/1.446545>.
- [33] D. Snoke and M. Cardona, Solid state communications **87**, 121 (1993).
  - [34] M. Yoshikawa, Y. Mori, M. Maegawa, G. Katagiri, H. Ishida, and A. Ishitani, Applied Physics Letters **62**, 3114 (1993).
  - [35] M. Yoshikawa, Y. Mori, H. Obata, M. Maegawa, G. Katagiri, H. Ishida, and A. Ishitani, Applied Physics Letters **67**, 694 (1995).
  - [36] M. Chaigneau, G. Picardi, H. A. Girard, J.-C. Arnault, and R. Ossikovski, Journal of Nanoparticle Research **14**, 955 (2012).
  - [37] O. I. Utesov, A. G. Yashenkin, and S. V. Koniakhin, arXiv preprint arXiv:2005.02937 (2020).
  - [38] S. V. Koniakhin, O. I. Utesov, and A. G. Yashenkin, arXiv preprint arXiv:2007.07086 (2020).
  - [39] O. A. Shenderova, I. I. Vlasov, S. Turner, G. Van Tendeloo, S. B. Orlinskii, A. A. Shiryaev, A. A. Khomich, S. N. Sulyanov, F. Jelezko, and J. Wrachtrup, The Journal of Physical Chemistry C **115**, 14014 (2011).
  - [40] T. Ando and Y. Uemura, Journal of the Physical Society of Japan **36**, 959 (1974).
  - [41] H. Haug and A.-P. Jauho, *Quantum kinetics in transport and optics of semiconductors*, vol. 2 (Springer, 2008).
  - [42] M. Stone, *Quantum Hall Effect* (World Scientific, 1992).
  - [43] J. T. Edwards and D. J. Thouless, Journal of Physics C: Solid State Physics **5**, 807 (1972), URL <https://doi.org/10.1088%2F0022-3719%2F5%2F8%2F007>.
  - [44] B. L. Altshuler, Y. Gefen, A. Kamenev, and L. S. Levitov, Phys. Rev. Lett. **78**, 2803 (1997), URL <https://link.aps.org/doi/10.1103/PhysRevLett.78.2803>.
  - [45] I. V. Gornyi, A. D. Mirlin, D. G. Polyakov, and A. L. Burin, Annalen der Physik **529**, 1600360 (2017), URL <https://onlinelibrary.wiley.com/doi/abs/10.1002/andp.201600360>.